Steady and dynamical analysis of a combined cooling and power cycle

N. Voeltzel, H.T. Phan, Q. Blondel, B. Gonzalez, N. Tauveron

Version of Record: https://www.sciencedirect.com/science/article/pii/S2451904920301700
Manuscript_626906c9d66d73f2e42537e2831241b4

Steady and Dynamical Analysis of a Combined Cooling and Power Cycle

N. Voeltzel[1,*], H.T. Phan[1], Q. Blondel[1], B. Gonzalez[1], N. Tauveron[1]
[*]Corresponding author, e-mail: nicolas.voeltzel@gmail.com

[1] Univ. Grenoble Alpes, CEA, LITEN, DTBH. F-38000 Grenoble, France

Abstract: Absorption cycles cogenerating cooling and power are anticipated to show favorable performances compared to separate generation systems. Through several models and a few prototypes, different studies validated the ability of cogeneration cycles to work with low-grade heat (lower than 200 °C). The present work aims to characterize and optimize a water-ammonia based cogeneration system of small capacity (cooling production: 5 kW, electricity production: 1 kW). Firstly, an accurate model of a scroll expander is implemented in a complete cogeneration cycle to simulate the power production. The effects on the expander of both the water/ammonia fraction and temperature of the expanded fluid are analyzed, providing a better understanding of the impacts of the rectifier and of the super-heater on the global cycle performances. Secondly, to foresee the cycle performance, a dual-objective optimization algorithm maximizes both cooling and power production according to variable temperature sources. Finally, the dynamic behavior of the cycle is investigated through transient simulations. Such complex systems present significant inertia when starting or switching from one production mode to another (between cooling and power). This study provides some insight on the most critical elements of the cycle.

Keywords: Power production; Cooling absorption cycle; Hybrid/cogeneration cycle; Scroll expander; Dual-objective optimization; Transient study

Nomenclature

Quantity	Symbol	Unit
Area	A	mm^2
Exchanged Heat	Q	J
Overall heat transfer coefficient	U	$W\ m^{-2}\ K^{-1}$
Temperature	T	°C
Efficiency	η	
Expander generated power	$\dot{W}$	kW
Mass flow rate	$\dot{m}$	$kg.s^{-1}$
Specific enthalpy	h	$kJ.kg^{-1}$
Friction coefficient	τ_{loss}	N
Split ratio	r_s	
Valve switching time	t_v	s

Quantity	Subscript
Expander	expa
Experimental	exp
Numerical	U
Expander inlet	in
Expander outlet	Out
Critical	c
Coefficient of Performance	COP
Combined Cooling and power	CCP
Organic Rankine Cycle	ORC
Hydrofluorocarbons	HFC
Built-in Volume Ratio	BVR

1. Introduction

The literature depicts various architectures of combined cooling and power (CCP) production. A first overview of the systems studied was proposed by Ayou *et al.* [1]. Two main families stand out: the cogeneration architectures in series [2–4] and those in parallel [5–7]. The architectures in series are generally more efficient for simultaneous co-generation of cooling and electricity while the architectures in parallel enable more flexibility to switch between production modes. Parallel architecture is also easier to implement because only two levels of pressure are present. Independently of the architectures, cooling can be produced through absorption chillers [3,5,6] or ejectors [2]. The combination of both technologies was also considered in several studies [7,8]. Electricity is produced

by the expansion of the working fluid in an expander (volumetric type or turbine) coupled to a generator. The development of expanders notably benefits from the recent study of organic fluid Rankine cycles (ORC) [9].

As cogeneration systems are quite complex cycles, only a few experimental investigations have been conducted so far and they usually simulate hard-provisioning components with simplified equivalents [5]. In return, the numerical approach is widely used to explore the performance of innovative architectures. Concerning cooling production, the physical models that describe the various components of thermodynamic cycles have already been well investigated and have led to numerous numerical studies of both absorption and compression machines [10]. Concerning power production, expander models need further investigation due to complex phenomena and a wide range of existing technologies.

Lemort *et al.* developed a first scroll expander model [11]. This semi-empirical model takes into account the physics related to the transformation of the fluid from the inlet to the outlet of a scroll. In CCP systems coupling an absorption cycle with an expander, the expanded gas in the expander is most often ammonia with traces of water. Hence, there is a real interest in adapting this model to work with ammonia. Based on experimental data, Mendoza et al. developed a simplified version of Lemort's model with ammonia as working fluid [12]. The model is later included into a CCP cycle and the performance of a scroll expander is then calculated for three different working fluids [6].

In line with literature work, the present study aims to characterize CCP cycles and optimize their performance. A parallel architecture of the expander integrated into an ammonia-water absorption chiller has been studied. Numerical models of the cycle were developed with a detailed model of a scroll-type expander. Tests were also conducted on the ORC and absorption-chiller machines available in our laboratory, giving experimental data for calibration of the model parameters and boundaries. The resulting steady and transient numerical simulations provide various information on the key factors affecting the cycle operation and its related performance.

2. Cycle description

The CCP cycle considered in the present study is shown in Figure 1. It consists of a water-ammonia absorption cycle, in parallel with an ORC cycle which use part of the desorbed ammonia as a working fluid and a scroll expander for power production.

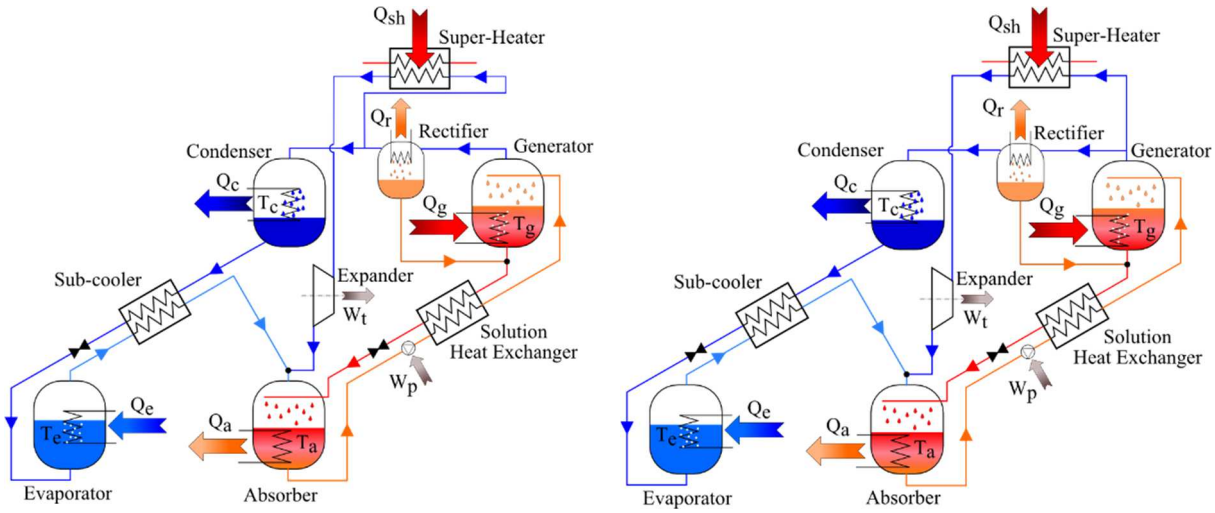

a) Configuration A b) Configuration B

Figure 1. Scheme of the CCP cycle with two different configurations.

On the solution circuit loop, a first line of ammonia-rich solution flows from the absorber to the generator through pressurization by a pump. A second line with an expansion valve brings the poor

solution back to the absorber. An economizer preheats the rich solution with the poor solution coming out of the generator.

Upstream of the production lines, a rectifier maximizes the ammonia content of the gas produced at the generator in order to obtain better performance for cooling production. In Configuration A (Figure 1), the rectification is effective for both the cooling and the power production lines, while in Configuration B the ammonia expended to produce power is not rectified as the switch valve directing the flow between the two production lines is positioned before the rectifier. The two variations of the cycle exist in different architectures present in the literature [5,6].

To produce power, a superheater raises the temperature of the fluid to ensure that it remains in a gaseous state throughout the expansion. In the scroll expander, the fluid is then trapped and expanded in expansion chambers. By deforming, the chambers cause the rotation of a shaft coupled to a generator to produce electricity.

To produce cooling, a heat exchange with an intermediate temperature source (usually the ambient) condenses the ammonia flowing from the generator. A valve expands the ammonia to low temperature so it can take calories at the evaporator and generate cooling. Finally, a subcooler allows the ammonia to be pre-cooled before it is expanded, by using the ammonia coming out of the evaporator.

The flows from the two production lines mix and are finally absorbed into the poor solution through cooling by a source of intermediate temperature (the same as the one used in the condenser).

3. Experimental devices

Two different devices provide data to setup the following numerical models: the scroll expander model is parametrized according to tests performed on an organic fluid Rankine cycles (ORC), and an absorption cycle prototype is characterized to setup the other components in the model of the complete CCP cycle.

3.1 Organic Rankine Cycle

Scroll expanders ensure the continuous expansion of a fluid in closed chambers. This solution is therefore very relevant for small power applications with moderate flow rates [13]. A 1 kW Air Squared® scroll expander (model E15H022A-SH) was mounted on an existing ORC test rig [14]. A preheater has also been added to the initial facility to increase the range of test conditions. In detail, a Hydra-Cell pump ensures the circulation and pressure elevation of the fluid. A preheater and an evaporator transfer up to 18 kW of thermal energy to it. Then the gaseous fluid expands in the scroll expander by driving a generator. Finally, a series of three condensers, fed by the same cold source, liquefy the fluid before it returns to the pump.

As ammonia cannot be directly tested in the installation, another pure fluid serves to characterize the scroll expander. The choice is an HFC commonly used in the heat pump industry: R245fa. This refrigerant have already demonstrated its ability to produce energy by expansion in an expander [15,16]. Thanks to adaptation laws between fluids described by [15], the characterization completed with R245fa allows to project the scroll behavior when operating with ammonia.

Conditions of operations tested on the ORC where chosen to be representative of the conditions expected in the combined cycle. Thus, the temperature of the heat source ranges from 90°C to 130°C as the high pressure of the cycle varies from 9 to 12 bar.

3.2 Absorption chiller

To characterize the other components in the studied CCP cycle, tests are performed on an existing water/ammonia absorption chiller device. This experimental cycle produces up to 5 kW of cooling (at temperature from -10°C to 20°C) from a heat source at low-grade temperature (70°C to 130°C) and a source at intermediate temperature (15°C to 45°C). The operating pressures vary between 8 and 20 bar on the high-pressure side and from 2 to 6 bar on the low-pressure side. Details of the design of the device and its detailed description were the subject of a previous paper [17]. In short, the operation of the device is identical to that of the CCP cycle studied and presented above without the electricity

production line parallel to the cooling production. The tests carried out on the device make it possible to estimate the pinches of temperature, pressure drops and efficiencies associated with the various components also present in the CCP cycle.

For both installations, the uncertainty of measurement of the temperature sensors is ±0.3 C and the ones of the flow rate sensors and pressure sensors are respectively 0.4 % and 1 %. Additionally, the measurement of produced electrical power on the ORC comes with 4 % of uncertainty.

4. Numerical Models

The two following models were implemented in the 'Engineering Equation Solver' (EES) environment to simulate the operations of the expander and cycles [18]. The calculated values of specific thermodynamic states come from EES's database for pure ammonia and water/ammonia mixtures.

4.1 Expander scroll modelling

Lemort's semi-empirical model [11] has been used in many studies to explore the different operating conditions of a scroll expander [12,15]. It quantitatively estimates the performance of an expander with a limited number of operating conditions (flow rates, pressures and temperatures) at the inlet. In detail, the model decomposes the flow of fluid through the scroll into seven distinct thermodynamic transformations. It also takes into account the mechanical and thermal exchanges of the scroll with its environment. The equations specific to each transformation and balance are detailed in the reference publication [11].

Table 1. Scroll properties determined from experimental data with R245fa. The bold values identify the corrections for operation with ammonia.

	A_{in} (mm²)	$AU_{in,n}$ (W/K)	$AU_{out,n}$ (W/K)	AU_{amb} (W/K)	BVR	A_{leak} (mm²)	τ_{loss} (N.m)
R245fa	28	12	31,4	7,5	2,7	5,7	0,2
Ammonia	28	**6**	**14,7**	7,5	**1,9**	**1**	0,2

The design of the expander, the working fluids and the operating conditions are inputs of the model. Table 1 lists the parameters related to the nature of the expander. A_{in} is the flow cross-section of the fluid at the expansion inlet. $AU_{in,n}$, $AU_{out,n}$ and AU_{amb} are the heat exchange coefficients of a fictitious isothermal wall with, respectively, the fluid before expansion, the fluid after expansion and the ambient. The Built-in Volume Ratio (BVR) characterizes the volume expansion rate. A_{leak} represents the total leakage area related to the flow of fluid through the expander that does not produce work. Finally, τ_{loss} is a mechanical friction coefficient.

The previous parameters are determined by minimizing the differences between experimental measurements and model calculations. The scroll response (power generation, output temperature and flow rate) was experimentally measured through 30 tests performed on the previously introduced ORC test bench for different temperature and flow rate conditions over the operating range of the expander. The same tests were simulated using the model by imposing four input parameters: the scroll speed, the temperature of the incoming fluid and the pressures upstream and downstream of the expander. The difference between the numerical and experimental results is quantified by the error ε:

$$\varepsilon = \sum \left[\left(\frac{T_{out,exp} - T_{out,num}}{\overline{T_{out,exp}}} \right)^2 + \left(\frac{\dot{W}_{exp} - \dot{W}_{num}}{\overline{\dot{W}_{exp}}} \right)^2 + \left(\frac{\dot{m}_{exp} - \dot{m}_{num}}{\overline{\dot{m}_{exp}}} \right)^2 \right] \qquad \text{(eq. 1)}$$

T_{out} , $\dot{W}$ and $\dot{m}$ are respectively the fluid temperature at the outlet, the power output and the fluid mass flow rate. The *exp* and *num* indices distinguish experimental quantities from numerically calculated quantities. A genetic algorithm is used to minimize the error ε and determine the values of the parameters listed in Table 1. To assess the accuracy of the model, a comparison is made between the

experimental measurements and the recalculated numerical values based on the newly determined parameters (Figure 2). It shows that the differences are less than 10% for 26 of the 30 configurations studied. The standard deviation over all configurations between the experimental and numerical data is 6 %, what tends to validate the numerical approach.

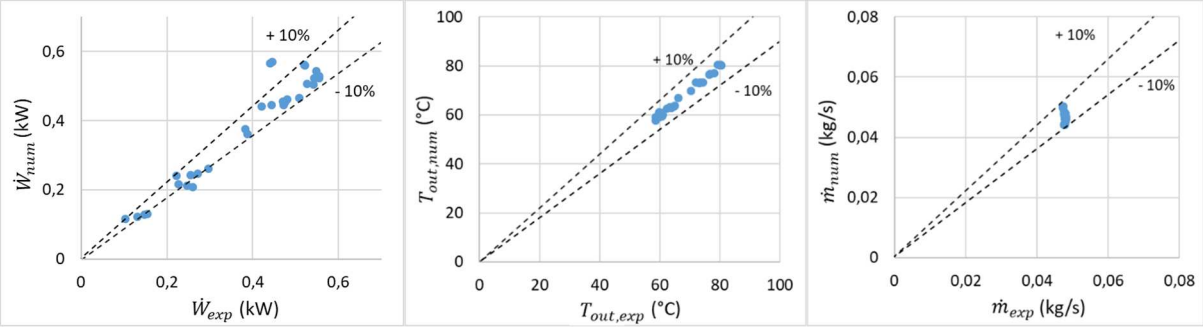

Figure 2. Comparison of numerical (vertical axis) and experimental (horizontal axis) results of $\dot{W}$, T_{out} and $\dot{m}$.

The heat exchange coefficients of the model depend on both the properties of the scroll and of the working fluid. In order to conserve the validity of a model calibrated on a type of scroll expander for different fluids, Giuffrida uses the intrinsic properties of the fluids to recalculate the heat exchange coefficients [15]. Thus, the values of the exchange coefficients $AU_{in,n}$ and $AU_{out,n}$ determined for R245fa take the values of 6 W/K and 15.7 W/K respectively with ammonia. The small variations of those coefficients caused by the presence of water in ammonia is neglected thereafter as the proportion of water is low (maximum 10% of the mixture) and the influence of the heat exchange on the global process is not predominant. Moreover, this scroll expender has already been tested with other zeotropic mixture, strengthening the assumption of regular operation with a fluid mixture [19].

The study of an expander designed to operate with ammonia also requires adapting its geometry to be compatible with the properties of the fluid. Thus, since the expansion rate of ammonia is significantly higher than that of R245fa, the BVR is reduced to 1.9 in the scroll expander model in order to keep a comparable pressure ratio

To evaluate the performance of the expander, its efficiency is defined as follows:

$$\eta_{expa} = \frac{\dot{W}}{\dot{m} . \Delta h_{is}} \qquad \text{(eq. 2)}$$

With Δh_{is} the enthalpy variation of the fluid in the scroll in the case of an isentropic transformation (ideal).

Considering the uncertainties of experimental measurements, the standard deviation between experimental and numerical values and the assumptions made on the change of fluid properties, we estimated the uncertainty of numerical calculations to be lower than 15%.

4.2 Modelling of the combined cooling and power cycle

A numerical model was developed based on the prototype of absorption cycle previously introduced. For each component, energy and mass conservation equations were written. The parameters of each heat exchanger (pinch, pressure drop and efficiency) were set with the values assessed experimentally on the water-ammonia absorption prototype [17]. Finally, it is assumed that the fluid is saturated at the outlet of each exchanger (except for an imposed superheating of 5 °C at the evaporator outlet). From this configuration, the model predicts the thermodynamic states anywhere in the cycle and the performance of the system for given operating conditions (temperature or power of the sources and solution mass flow rate).

To complete the development of the CCP cycle, the scroll expander model is integrated into the absorption chiller model, in parallel of the cooling production line (see Figure 1). In addition, a superheater modelled as an adjustable power supply to the fluid precedes the scroll. In order to control the share of cooling and electricity production, the split ratio r_s divides the refrigerant flow between the two production lines. It is equal to the ratio of the mass flow rate of ammonia passing through the

evaporator to the mass flow rate of ammonia produced at the generator. In most of the following study, the split ratio r_s is set to 0.5, so distribution of generated ammonia is fair between the two production lines.

To estimate the cooling production efficiency of the CCP cycle, the COP is defined as follows:

$$COP = \frac{Q_{evap}}{Q_{gen}.r_s} \qquad \text{(eq.3)}$$

With Q_{evap} the thermal power exchanged at the evaporator and Q_{gen} the thermal power exchanged at the generator.

4.3 Multi-objective genetic algorithm

A CCP cycle can produce power and cooling alternatively or simultaneously, but the optimal operational conditions for each production might not be the same. In addition, the quantification of each production is not directly comparable as the cooling thermal power is generally much higher in standard unit of power than the mechanical/electrical power. Therefore, an optimization algorithm that independently considers the power and the cooling production is necessary to perform a relevant optimization of the operational settings.

In 2002, Deb et al. developed a reputed multi-objective genetic algorithm based on a nondominated sorting approach (NSGA-II) [20]. This optimization algorithm enables to maximize the simultaneous productions of cooling and power by determining a pareto-like maximization front for optimized operating conditions of the CCP cycle. In this study, the NSGA-II algorithm is coupled to the EES solver software using a loop strategy. A population of model input sets (individuals) is generated by the genetic algorithm, EES tests them and return the resulting power and cooling productions for each input set, finally the genetic algorithm treats them to generate a more accurate new generation of input set to be tested. A criterion of 5.10^{-3} residual variation of the maximized values of the algorithm population is implemented to stop the optimization loop.

5. Results and discussion

A first analysis focuses on the operation of the scroll expander under the operating conditions of a CCP cycle and defines a newly criteria to assess the quality of volumetric expanders. Then we explore the performance of the complete cycle and carry out a comparative study between the two configurations of the cycle presented in Figure 1. Next, a dual-objective optimization presents the potential of cooling and power production of the cycle according to the temperatures of the sources. Finally, a transient study of the cycle introduces the dynamical inertia inherent to this complex system.

5.1 Performance and sizing of an expander operating in the conditions of a CCP cycle

In a conventional absorption cycle, the flow of ammonia produced at the generator matches 20-30% of the flow of rich solution [10]. More precisely, tests on the absorption chiller prototype estimate a maximum flow rate of fluid through the expander of about 0.01 kg/s. Figure 3 shows the power production of the scroll with ammonia as a function of the flow rate. In order to highlight the sensitivity of the scroll performance to the low flow rate imposed by the CCP cycle (~ 0.01 kg/s), the study focuses on the influence of the following sensitive parameters: the pressure variation in the expander ΔP and the leakage area A_{leak}. We note that for a leakage area equivalent to that determined for the expander installed on the ORC test rig (solid curves), energy production is nil or very low for flow rates below 0.01 kg/s. In this configuration, the internal leakages are too important compared to the ammonia flow and the scroll is not being driven. This effect is even more important with higher differential pressure in the scroll (bold curves).

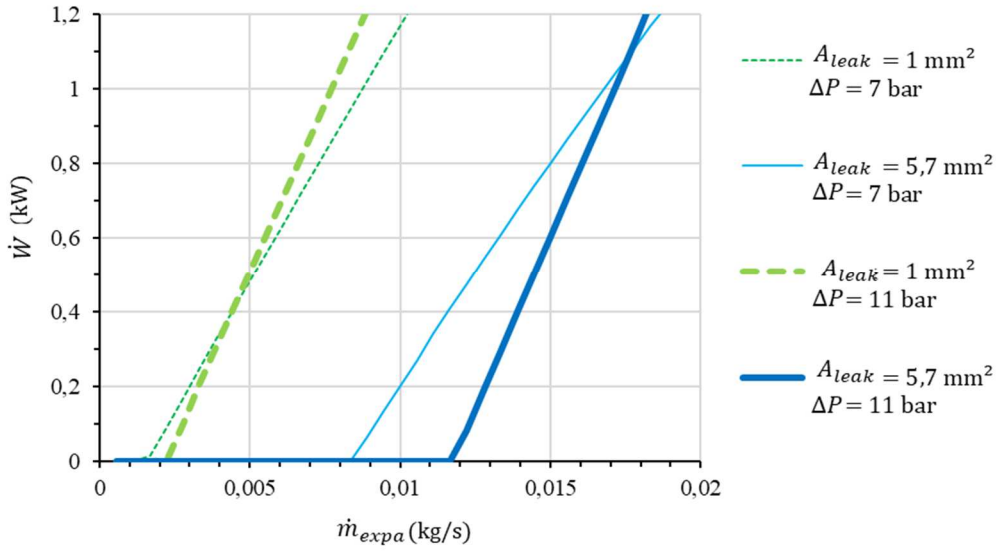

Figure 3. Mechanical power produced by the scroll expander as a function of the leakage area and the pressure variation in the expander.

With a leakage area reduced to 1 mm², the critical flow rate required to produce power is reduced to about 0.003 kg/s (dotted curves). As the leakage area is directly related to the volume efficiency of scroll expanders, this result illustrates the need to design highly efficient expanders with small leakage area for the development of small capacity CCP cycles. Accordingly, a reduced leakage area of A_{leak}= 1 mm² is retained for the rest of the study to simulate an expander with an acceptable efficiency.

The characterization of leaks in expanders operating with ammonia is of major concerns as there are essential in the development of CCP cycle, Kalina cycle [21] or ORC operating with ammonia. Considering a critical leakage area $A_{leak,c}$ being the limit for A_{leak} above the one there is no power generation, it is relevant for expander constructors to evaluate this critical area easily from the foreseen operating conditions. The equations that govern the leaks in Lemort *et al.* publication [11] involve numerous parameters. Through a sensitivity analysis of these equations, we stated that, in addition to the fluid nature, mostly the leakage area and the upstream pressure influence the leakage mass flow rate. An evaluation of the leak evolution, with variations of these two last parameters, enable to identify an analytical law to predict the critical mass flow rate:

$$A_{leak,c} = k\frac{\dot{m}_{expa}}{P_{in}} \qquad \text{(eq. 4)}$$

With k a constant consistent with speed unit and proper to the fluid. A regression of the mean square deviation between the law and the numerical prediction gives a value of k = 612.3 m/s for ammonia as working fluid. Finally, the prediction of the analytical law (eq. 4) fits with the numerical calculation of a critical leakage area with less than 3.7 % of relative error (see Figure 4).

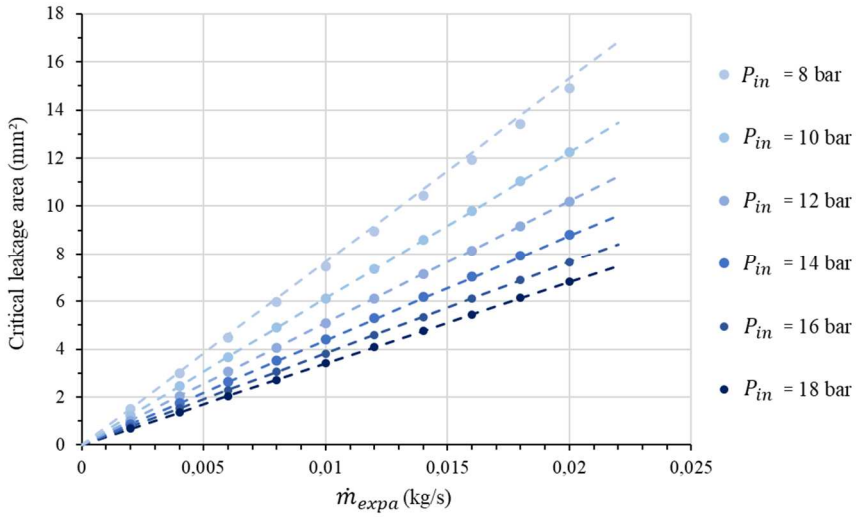

Figure 4. Numerical and analytical calculations of the critical leakage area of a scroll expander as a function of the ammonia mass flow rate and the pressure differential through the scroll.

The numerical data are computed for an inlet temperature of the fluid in the turbine of 110 °C and an outlet pressure of 4 bar. Nonetheless, sensitivity calculations show that the leakage mass flow rate varies less than 11 % for an input temperature between 90° and 160°C, with a slight leakage decrease when the temperature increases. Moreover, the outlet pressure doesn't act on the leakage numerical calculation unless it is greater than about 50 % of the inlet pressure, what is very rarely the case in ammonia absorption chiller. Thus, the scope of validity of the analytical law to estimate a critical leakage area (eq. 3) cover a large range of CCP cycles empowered by low-grade temperature source (90°C to 160°C).

5.2 Influence of the position of the rectifier in the CCP cycle

To compare the two configurations of cycles previously introduced (see Figure 1), we analyzed the action of the rectifier on the cycle performance. By lowering the temperature of the gas produced at the generator, the rectifier will condense the remaining traces of water in the gaseous ammonia and redirect them to the poor solution. Thus, the rectifier limits the water content in the ammonia, but also reduces the flow rate of downstream components on cooling and power production lines. To quantify the overall influence of the rectification on cycle efficiencies, Figure 5 shows, for both configurations, the expander efficiency (eq. 2) and the COP (eq. 3) of the cooling production as a function of the mass fraction of ammonia in the evaporator. For the comparison, the cycle inputs are set as follow to reconcile optimal performance of the cycle and realistic conditions of operation: the rich solution flow rate is set to 0.028 kg/s ; the superheater imposes an increase of temperature of 15°C between the generated ammonia and scroll inlet ; the sources of hot, intermediate and cold temperatures are set respectively to 110°C, 27°C and 18°C and representative of low-grade heat source, warm ambient temperature and moderate cooling production for air conditioning units. The study remains valid for reasonable variation of those input as the described following phenomena are not directly connected to them.

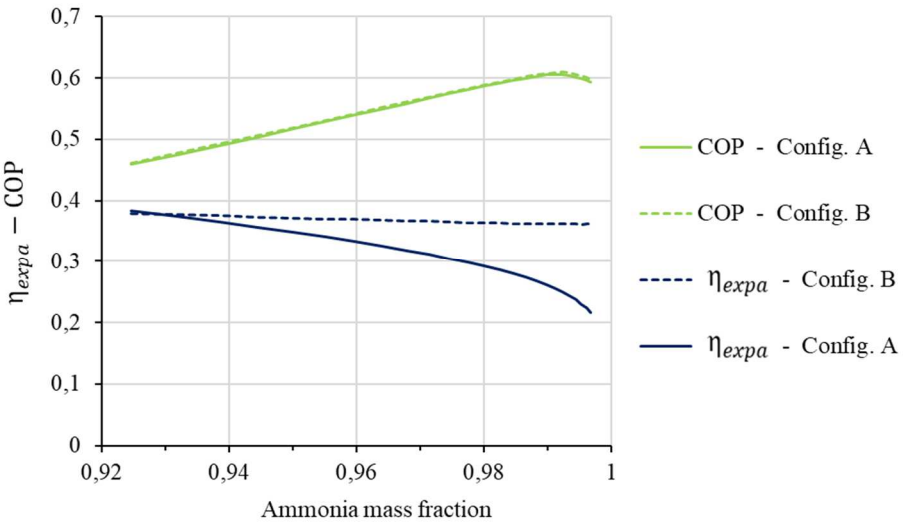

Figure 5. Expander efficiency and COP of the cooling production as a function of the mass fraction of ammonia at the evaporator.

The results confirm the relevance of the rectifier to improve the performance of cooling production as the COP increases to an optimum corresponding to an ammonia content of 99.2%. In addition, it can be observed that the COP is logically relatively unaffected by the cycle configuration since in both configurations the rectifier is always upstream of the cooling production line.

Focusing on the power production, the rectification of ammonia before it passes through the expander (configuration A) results in a significant decrease of the expander efficiency. An optimal rectification of cooling generation, corresponding to a mixture with 99.2% ammonia, leads to 34% reduction of the scroll efficiency. This trend does not occur when the ammonia entering the expander is not rectified (configuration B). The decrease of the expander efficiency is then limited to 5% and is only caused by the reduction of the high pressure of the cycle, the one driven by the rectification rate occurring on the cooling production line.

The rectification of the ammonia solution intended for power production causes two effects that have opposite influences on the expander efficiency. Firstly, rectification increases the ammonia rate of the solution, and with it its volume expansion coefficient (representative of the gas volume variation for a given variation of pressure) [18]. This tends to improve the expander efficiency as it increases the displacement of the expander movable parts for a given flow rate. Secondly, rectification reroutes part of the generated ammonia solution and it has just been seen in the previous section that a lower flow rate reduces the expander efficiency.

Finally, the global reduction of expander efficiency caused by the rectification as shown in Figure 5 makes it possible to establish that the loss of performance attributable to the presence of water vapor in the working fluid is less significant than that due to the reduction in flow rate caused by the rectification.

Note that other constraints (serial CCP cycle, combined generator-rectifier, etc.) may favor the choice of a less optimal configuration (type configuration A). Hence, the previous quantified comparison can help as a preliminary study to arbitrate between different architectural options.

5.3 Dual optimization of the power and cooling production

In this section, the most efficient configuration of the CCP cycle is considered (see Configuration B, Figure 1). The multi-objective genetic algorithm previously described is operated to maximize the simultaneous productions of cooling and power. The three temperatures of the sources are the optimizable parameters and the only fixed input is the power exchanged at the generator that is set to 10 kW. The temperatures have the same boundaries than that of the absorption-chiller test bench as described in a previous section. The pressures and the mass flow rates are all outputs of the modelling.

The setting of the genetic algorithm is as follow: populations of 1000 individuals, crossover probability of 0.9 and mutation probability of 0.1. 50 generations are necessary to achieve a 5.10^{-3} residual variation of the maximized values of the algorithm population.

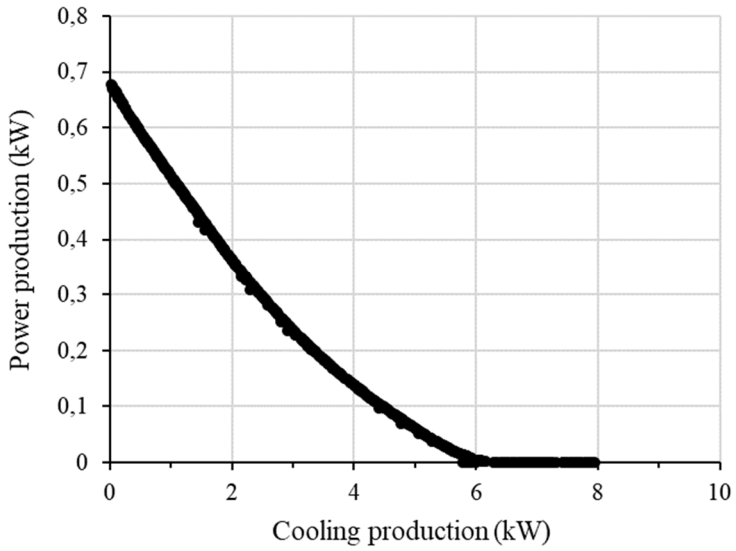

Figure 6. Optimum frontier of the cooling and power productions obtained through a dual-optimization algorithm.

The graph on Figure 6 displays the optimum frontier obtained through the calculation of the dual-objective optimization. First, it informs that, functioning alternatively, the cycle can produce up to 680 W of power and 8 kW of cooling. Between these two extreme production modes, the plotted results show the maximum power and cooling production that can be produced simultaneously. One can notice that no power can be produced for cooling production greater than 6 kW. This limitation is directly related to the mass flow rate passing through the expander. As cooling and power productions are set in parallel in the cycle, the flow rate through the expander decreases with increasing cooling production and, as previously presented, this one becomes too low to get over the leakage of fluid through the expander.

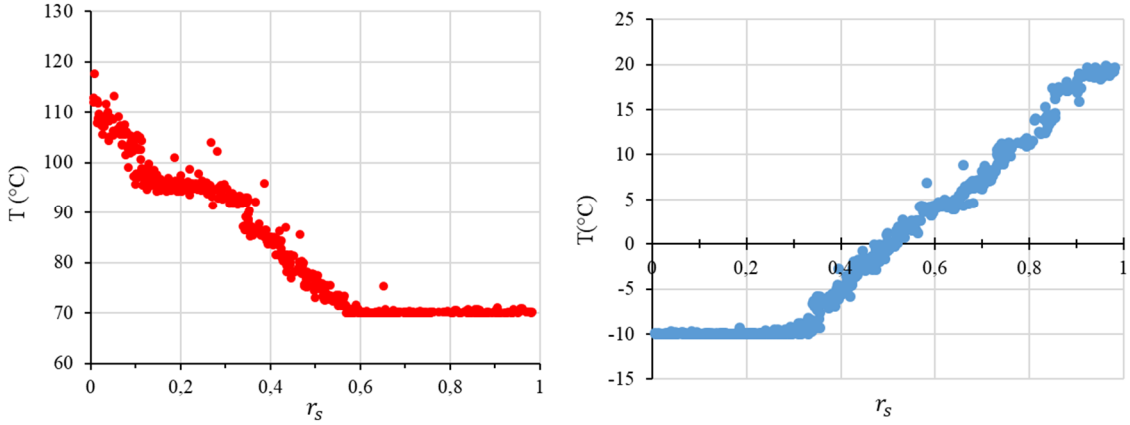

Figure 7. Evolution of the temperatures of the hot source (left) and of the cooling production (right) with the split ratio determined by to the dual-optimization algorithm.

The graphs on Figure 7 display the evolution of both temperatures of hot source and cooling production from power production alone (split ratio $r_s = 0$) to cooling production alone ($r_s = 1$) and for all the in-between simultaneous production modes. It shows that the hot source temperature is preferentially higher for power production and lower for cooling production, while the opposite is observed for the cooling production temperature. The plateaus are a consequence of the imposed

boundaries for the temperatures of the sources. Those behaviors can directly be explained by the influence of the temperature on the operating pressures and mass flow rates and on the expansion potency of the ammonia that increases with the temperature. The results are also consistent with the preliminary experimental observations on both test benches.

5.4 Transient analysis of varying production of power and cooling

To complete the study, a dynamic model of the CCP cycle based on the previously used steady one is developed in the dynamic solver Dymola®. The objective is to foresee characteristic response times and potential instability of the cycle when changing the production mode to adapt the generation of cooling and power to the user needs. This analysis will then help to configure an efficient predictive control of the system. Some simplifications were made to the dynamic model to accelerate the calculation time of the simulations and to gives the possibility to explore various scenarios. Hence, the rectification and the sub-cooler system are not present in the dynamic modelling, and the expander is modelled via a constant isentropic efficiency of 38% and an imposed rotational speed of 60 Hz as if connected to a national electrical grid.

Figure 8 illustrates for two transient scenarios the typical response times of the power and cooling productions to a change of control of the three-way valve dividing the ammonia flux in the production lines. In the first setup, the split ratio r_s starts at a steady value of 0.5, corresponding to a simultaneous production of cooling and power. From $t = 0$, the operating control changes to reach $r_s = 0$ (i.e. power production alone). In the second setup, the split ratio r_s starts at a steady value of 0 and from $t = 0$, the operating control changes to reach $r_s = 1$ (i.e. cooling production alone). To match the behavior of classic automated valves, the valve switching time t_v is set to 20 seconds in the first scenario and 30 seconds in the second one.

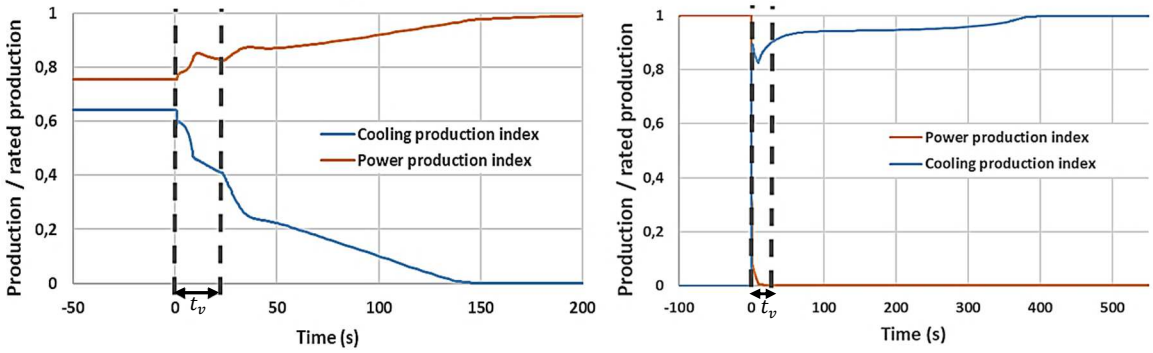

Figure 8. Evolution of the productions of cooling and power after a change of the controlling inputs. From a mix of both productions to power production alone (left) and from power production alone to cooling production alone (right).

The first important observation is that there is no important instability of the system when switching from a production mode to another. The dynamic simulations predict that the transitions are not systematically instant, but they are always smooth enough to guarantee the stability of the system.

When switching from a mix production mode to a power production alone mode, a transient phase occurs before the cooling production stops and the power production reaches its nominal value. This is mainly the consequence of the condenser and evaporator inertia. In fact, both heat exchangers partly contain liquid ammonia when cooling production is operating, so when the valve closes before the condenser, this ammonia will take time to evaporate as low pressure of the cycle decreases. The symmetrical increase of power production is a consequence of the lowering low pressure that implies an increase of the pressure ratio at the expander ends. In the present simulation, this transient state last about two minutes and this time will be directly correlated to the volumes of the heat exchangers.

In the second scenario, when switching to power production alone to cooling production alone, the power production stops instantaneously as there is no storage of ammonia before the expander and the flow is immediately nil. The initialization of cooling production is instant too, but it takes about 6

minutes to reach the optimal cooling production as the heat exchangers takes time to reach their liquid/vapor equilibrium.

6. Conclusion

Among the CCP cycle architectures under development, those in parallel are the most versatile and easiest to implement but they have not been widely investigated. To contribute to the development of these systems, a complete numerical model of the parallel CCP cycle was developed and configured through the characterization of two experimental devices: an ORC test rig to characterize a scroll expander and an absorption cycle to evaluate the rest of the system.

Early results highlighted the importance of using a detailed expander model to quantify the intrinsic physics of the flows in the scroll. Indeed, under the operating conditions of a small capacity machine, low flow rates require the use of expanders of high volumetric efficiency. Moreover, an analysis focusing on the role and position of the rectifier in the cycle highlights its influence on the performance of power production. This result introduces a new criterion for cycle architecture optimization. To go further, a dual-objective optimization algorithm highlighted the potential of the CCP cycle and introduced some leanings to optimize the operating conditions according to the different production modes. Finally, dynamic simulations of a combined cooling and power cogeneration system predict that the transition between production modes are quite stable and that the transition times are longer when starting power production than when starting cooling production.

7. Acknowledgments

The French Alternative Energies and Atomic Energy Commission (CEA) and Carnot Energies du Futur supported this work.

8. References

[1] D.S. Ayou, J.C. Bruno, R. Saravanan, A. Coronas, An overview of combined absorption power and cooling cycles, Renew. Sustain. Energy Rev. 21 (2013) 728–748. https://doi.org/10.1016/j.rser.2012.12.068.

[2] A. Khaliq, Energetic and exergetic performance investigation of a solar based integrated system for cogeneration of power and cooling, Appl. Therm. Eng. 112 (2017) 1305–1316. https://doi.org/10.1016/j.applthermaleng.2016.10.127.

[3] J. Muye, D.S. Ayou, R. Saravanan, A. Coronas, Performance study of a solar absorption power-cooling system, Appl. Therm. Eng. 97 (2016) 59–67. https://doi.org/10.1016/j.applthermaleng.2015.09.034.

[4] F. Xu, D. Yogi Goswami, S. S. Bhagwat, A combined power/cooling cycle, Energy. 25 (2000) 233–246. https://doi.org/10.1016/S0360-5442(99)00071-7.

[5] G.P. Kumar, R. Saravanan, A. Coronas, Experimental studies on combined cooling and power system driven by low-grade heat sources, Energy. 128 (2017) 801–812. https://doi.org/10.1016/j.energy.2017.04.066.

[6] L.C. Mendoza, D.S. Ayou, J. Navarro-Esbrí, J.C. Bruno, A. Coronas, Small capacity absorption systems for cooling and power with a scroll expander and ammonia based working fluids, Appl. Therm. Eng. 72 (2014) 258–265. https://doi.org/10.1016/j.applthermaleng.2014.06.019.

[7] J. Wang, Y. Dai, T. Zhang, S. Ma, Parametric analysis for a new combined power and ejector-absorption refrigeration cycle, Energy. 34 (2009) 1587–1593. https://doi.org/10.1016/j.energy.2009.07.004.

[8] G.K. Alexis, Performance parameters for the design of a combined refrigeration and electrical power cogeneration system, Int. J. Refrig. 30 (2007) 1097–1103.

https://doi.org/10.1016/j.ijrefrig.2006.12.013.

[9] N. Tauveron, S. Colasson, J.A. Gruss, Available systems for the conversion of waste heat to electricity, in: Proc. ASME 2014 Int. Mech. Eng. Congr. Expo., 2014: pp. 1–12. https://doi.org/10.1115/IMECE2014-37984.

[10] K. Herold, R. Radermacher, S. Klein, Absorption Chillers and Heat Pumps, Second Edition, (2016). https://doi.org/10.1201/b19625.

[11] V. Lemort, S. Quoilin, C. Cuevas, J. Lebrun, Testing and modeling a scroll expander integrated into an Organic Rankine Cycle, Appl. Therm. Eng. 29 (2009) 3094–3102. https://doi.org/10.1016/j.applthermaleng.2009.04.013.

[12] L.C. Mendoza, J. Navarro-Esbrí, J.C. Bruno, V. Lemort, A. Coronas, Characterization and modeling of a scroll expander with air and ammonia as working fluid, Appl. Therm. Eng. 70 (2014) 630–640. https://doi.org/10.1016/j.applthermaleng.2014.05.069.

[13] A. Landelle, N. Tauveron, R. Revellin, P. Haberschill, S. Colasson, Experimental Investigation of a Transcritical Organic Rankine Cycle with Scroll Expander for Low - Temperature Waste Heat Recovery, in: Energy Procedia, Elsevier B.V., 2017: pp. 810–817. https://doi.org/10.1016/j.egypro.2017.09.142.

[14] A. Landelle, N. Tauveron, R. Revellin, P. Haberschill, S. Colasson, V. Roussel, Performance investigation of reciprocating pump running with organic fluid for organic Rankine cycle, Appl. Therm. Eng. 113 (2017) 962–969. https://doi.org/10.1016/j.applthermaleng.2016.11.096.

[15] A. Giuffrida, Modelling the performance of a scroll expander for small organic Rankine cycles when changing the working fluid, Appl. Therm. Eng. 70 (2014) 1040–1049. https://doi.org/10.1016/j.applthermaleng.2014.06.004.

[16] S. Declaye, S. Quoilin, L. Guillaume, V. Lemort, Experimental study on an open-drive scroll expander integrated into an ORC (Organic Rankine Cycle) system with R245fa as working fluid, Energy. 55 (2013) 173–183. https://doi.org/10.1016/j.energy.2013.04.003.

[17] F. Boudéhenn, H. Demasles, J. Wyttenbach, X. Jobard, D. Chèze, P. Papillon, Development of a 5 kW cooling capacity ammonia-water absorption chiller for solar cooling applications, Energy Procedia. 30 (2012) 35–43. https://doi.org/10.1016/j.egypro.2012.11.006.

[18] S.A. Klein, Development and integration of an equation-solving program for engineering thermodynamics courses, Comput. Appl. Eng. Educ. 1 (1993) 265–275. https://doi.org/10.1002/cae.6180010310.

[19] G. Bamorovat Abadi, E. Yun, K.C. Kim, Experimental study of a 1 kw organic Rankine cycle with a zeotropic mixture of R245fa/R134a, Energy. 93 (2015) 2363–2373. https://doi.org/10.1016/j.energy.2015.10.092.

[20] K. Deb, A. Pratap, S. Agarwal, T. Meyarivan, A fast and elitist multiobjective genetic algorithm: NSGA-II, IEEE Trans. Evol. Comput. 6 (2002) 182–197. https://doi.org/10.1109/4235.996017.

[21] P.K. Nag, A.V.S.S.K.S. Gupta, Exergy analysis of the kalina cycle, Appl. Therm. Eng. 18 (1998) 427–439. https://doi.org/10.1016/S1359-4311(97)00047-1.